

Yuxin YAO, Yujin HAO, Ming LI, Mingli PANG, Zhi LIU, Heng ZHAI

Gene clone, expression and enzyme activity assay of a cytosolic malate dehydrogenase from apple fruits

© Higher Education Press and Springer-Verlag 2008

Abstract Malate dehydrogenase (MDH) ubiquitously exists in animals, plants and microorganisms, and catalyzes the interconversion from oxaloacetate to malate. Cytosolic NAD-dependent MDH gene (*cyMDH*) encodes a key enzyme crucial for malic acid synthesis in the cytosol which has not been extensively characterized in plants. In this study, a full-length cDNA of *cyMDH* was isolated from apple fruits with RT-PCR as well as 3' and 5' rapid amplification of cDNA ends, and designated as *Mal-cyMDH* (GenBank accession No. DQ221207). It contained a 996-bp ORF and its sequence analysis shows a high similarity to other plant cyMDHs. Phylogenetic analysis indicated that almost all the cyMDHs could be clustered into the same group and it was likely to represent the original MDH. A roughly 37-kDa fused protein was obtained by the recombinant prokaryotic expression and its enzyme activity assay showed that it mainly catalyzed oxaloacetate to malate. It was also discovered that the enzyme activity of cyMDH exhibited remarkable difference between the high- and low-acid apple germplasm.

Keywords apple, cytosolic malate dehydrogenase, gene clone, prokaryotic expression, enzyme activity

1 Introduction

Malate dehydrogenase (MDH) is a highly conserved, ubiquitous enzyme in bacteria, fungi, plants and animals. MDH catalyzes the reversible reaction from oxaloacetate (OAA) to malate associated with the oxidation/reduction of dinucleotide coenzymes. All plant and mammalian

MDHs as well as the most bacterial MDHs are homodimers. The relative molecular mass is 32–37 kDa for NAD-dependent MDHs, while it is 42–43 kDa for NADP-dependent ones. MDHs play crucial roles in several metabolic pathways such as catabolic and anabolic metabolism. Higher plants produce a variety of MDHs with different co-enzyme specificity, subcellular localization and physiological function. Generally, plant MDHs can be divided into five classes, i.e., Chloroplast NADP-dependent MDH, Mitochondrial NAD-dependent MDH, Microbody NAD-dependent MDH, Chloroplast NAD-dependent MDH and Cytosolic NAD-dependent MDH (*cyMDH*) (Yu and Ma, 2004). Chloroplast NADP-dependent MDH, mitochondrial NAD-dependent MDH and microbody NAD-dependent MDH isoforms have been extensively investigated and well documented in plants. However, little is known about the other MDH isoforms, especially cytosolic NAD-dependent MDH (*cyMDH*).

It is deemed that *cyMDH* is involved in the exchange of substrates and reducing equivalents between cytoplasm and cellular organelles as part of various shuttle systems (Kromer and Heldt, 1991; Hanning and Heldt, 1993; Yu and Ma, 2004). *cyMDH* is also important for gluconeogenic function *in vivo* in yeast (Gibson and McAlister-Henn, 2003) and confers nucleic acid selectivity of the channel (Basil et al., 2002). In addition, *cyMDH* is one of the key enzymes involved in malic acid metabolism responsible for catalyzing the synthesis of malic acid with phosphoenolpyruvate carboxylase (PEPC) in the cytosol (Chollet et al., 1996). So far, there are no other reports about the relationship between *cyMDH* transcript and malic acid accumulation, except for the report in peaches (Christelle et al., 2002). Apples mainly accumulate malic acid during the development, so it is the best material for the research on the relationships between *cyMDH* transcript, enzyme activity and malic acid content. cDNA sequences of malate dehydrogenase (MDH) were cloned from various species. To the best of our knowledge, however, *cyMDH* was isolated only from peaches (Christelle et al., 2002). Here, we report the isolation and prokaryotic

Translated from *Acta Horticulturae Sinica*, 2008, 35(2): 181–188 [译自: 园艺学报]

Yuxin YAO, Yujin HAO, Ming LI, Mingli PANG, Zhi LIU, Heng ZHAI (✉)

State Key Laboratory of Crop Biology, College of Horticultural Science and Engineering, Shandong Agricultural University, Tai'an 271018, China

E-mail: yaoyx@sdau.edu.cn

expression of *cyMDH* from apples and analyze the effects of *cyMDH* activity on the malic acid content.

2 Materials and methods

2.1 Plant materials

The high- and low-acid hybrids of 'Toko' × 'Fuji' (*Malus × domestica* Borkh.) were selected in the experimental orchard of the Liaoning Institute of Fruit Tree Science (Liaoning, China). Fruit tissues were collected at 7, 30, 60, 75, 90, 120 and 150 days after full bloom (DAB) and then were immediately frozen in liquid nitrogen and stored at -80°C for RNA and enzyme extraction.

2.2 Malic acid analysis

Four fruits were picked from each hybrid at the corresponding developmental stages. Equal weights of flesh was collected and mixed. Malic acid contents were tested with capillary electrophoresis: uncoated capillary ($50\ \mu\text{m} \times 57\ \text{cm}$); Applied voltage: 10 kV; injection time: 3 s; $\lambda = 200\ \text{nm}$; Temperature: 20°C ; $100\ \text{mmol}\cdot\text{L}^{-1}\ \text{K}_2\text{HPO}_4 + 0.5\ \text{mmol}\cdot\text{L}^{-1}\ \text{CTAB}$; $\text{pH} = 7$.

2.3 cDNA cloning

Total RNA was isolated from the apple fruit with the modified hot borate method (Yao et al., 2005). Two micrograms of total RNA was used to synthesize the first-strand cDNA with M-MLV RTase cDNA Synthesis Kit (Takara, China). A partial *Mal-cyMDH* fragment was obtained by RT-PCR using degenerate primers: 5'-GTT CGY GTY CTY GTY ACY GG-3' (forward, *Mal-cyMDH-F*), 5'-CTN ACY GNC CRT NAY GAN TG-3' (reverse, *Mal-cyMDH-R*). The amplified fragment was sequenced and compared with the *cyMDH* of other plants to confirm whether it was the *cyMDH* homologue. The flanking 3'- and 5'- regions were obtained using the rapid amplification kit of cDNA ends (Takara, China).

2.4 Sequence alignment and phylogenetic analysis

Amino acid sequences were aligned using the Clustal W multiple alignment program. The phylogenetic tree was generated by the megalign program of the DNASTAR software. Sequences can be found at <http://www.ncbi.nlm.nih.gov>.

2.5 Functional expression of *Mal-cyMDH* in *E. coli*

PCR was used to introduce *Bam*HI and *Sal*I sites at the ATG start codon and TAG stop codon of *Mal-cyMDH*

coding region, respectively. The 5'- and 3'-primers used were: 5'- GCG GAT CCA TGG CGA AAG AAC CAG TTC-3' and 5'-GCG TCG ACA GTC GAA GTG TCC GAA TAG AAT-3', respectively. The fidelity of the PCR amplification was confirmed by DNA sequencing. The amplified product was digested with *Bam*HI and *Sal*I and cloned into a similarly digested pET-30a-c(+) expression plasmid. The resulting plasmid, pET30-*cyMDH*, was transformed to *E. coli* BL21(DE3). The bacterial cells were grown at 37°C and then induced by $0.5\ \text{mmol}\cdot\text{L}^{-1}$ IPTG at different temperatures. Proteins were separated on 12% SDS-PAGE.

2.6 Purification of recombinant Mal-*cyMDH* protein and assay of enzyme activity

All purification steps were carried out at 4°C . The bacterial culture was grown at 37°C until $A_{600} = 0.7$ and was then moved to 16°C with shaking for 1 h. IPTG was then added to the final concentration of $0.5\ \text{mmol}\cdot\text{L}^{-1}$ and the cells were cultured at 16°C for 24 h. Induced *E. coli* cells were pelleted at $2000 \times g$ for 10 min and resuspended in an extraction buffer ($50\ \text{mmol}\cdot\text{L}^{-1}$ Tris-HCl, $\text{pH} 8.5$, $500\ \text{mmol}\cdot\text{L}^{-1}$ NaCl, 10% glycerol, 1% Triton X-100, $20\ \text{mmol}\cdot\text{L}^{-1}$ mercaptoethanol and $1\ \text{mmol}\cdot\text{L}^{-1}$ PMSF). After the addition of lysozyme to $100\ \mu\text{g}\cdot\text{mL}^{-1}$, the cells were incubated at 30°C for 15 min. Cells were sonicated $3 \times 2\ \text{min}$ at 20 cycles per minute and extracts were then spun at $15000 \times g$ for 15 min. The supernatant was used for further purification using Ni-NTA His-Bind Resin (Novagen, USA) according to the manufacturer's instructions. Protein concentrations were determined by Coomassie brilliant blue G-250 using BSA as a standard (Bradford et al., 1976).

CyMDH enzyme activity was assayed spectrophotometrically at 340 nm. For each reaction, 6 min of spectrophotometrical change at A_{340} was monitored automatically at 1-min intervals. For the determination of the kinetic parameters for oxaloacetate (OAA), NADH, malate and NAD^+ , the respective fixed co-substrate concentrations were $0.2\ \text{mmol}\cdot\text{L}^{-1}$ NADH, $0.5\ \text{mmol}\cdot\text{L}^{-1}$ OAA, $1.0\ \text{mmol}\cdot\text{L}^{-1}$ NAD^+ and $50\ \text{mmol}\cdot\text{L}^{-1}$ L-malate. Assays were carried out in a 3-mL reaction volume in $50\ \text{mmol}\cdot\text{L}^{-1}$ MOPS ($\text{pH} 7.9$) buffer. The slope from *x*-axis by time and *y*-axis by absorption value is the enzymatic reaction speed ($\text{OD}\cdot\text{min}^{-1}\cdot\text{mg}^{-1}\text{Pr}$). Then, the unit was converted to $\mu\text{mol}\cdot\text{L}^{-1}\cdot\text{min}^{-1}\cdot\text{mg}^{-1}\text{Pr}$ by the standard curve of NADH. Every reaction was repeated three times.

2.7 Cytosolic enzyme extraction and assay of *cyMDH* activity

All operations were carried out at $0-4^{\circ}\text{C}$. Frozen (-80°C) apple flesh (5 g) at five developmental stages were ground to fine powder together with 1% (w/v) PVPP in a Waring blender. The powder was then homogenized for 1h after

adding 5 mL of extraction buffer containing 100 mmol·L⁻¹ MOPS, pH 8.0, 1 mol·L⁻¹ NaCl, 250 mmol·L⁻¹ sucrose, 100 mmol·L⁻¹ bicine, 2 mmol·L⁻¹ EDTA-NaOH, pH 8.0, 0.2 mmol·L⁻¹ MgSO₄, 0.75 mg·mL⁻¹ BSA and 1% (w/v) PVPP. The homogenized sample was filtered through double layers of Miracloth (Calbiochem, Damstadt, Germany) and then centrifuged at 2800 × g for 20 min. The debris was discarded followed by another centrifuge at 100000 × g for 1h in a Bechmann J30i ultracentrifuge. The supernatants were then de-salted by extensive dialysis against sterile distilled water. Aliquots of the extracts were then stored at -80°C for activity assay. The method of enzyme assay is introduced in section 2.6.

3 Results

3.1 Isolation of Mal-cyMDH and sequence alignment

PCR amplification with the degenerate primers yielded a 705-bp product from apple fruit cDNA. 5' and 3' RACES were used to amplify the flanking regions. The result indicated a 1246-bp cDNA including an ATG start codon, a TAG stop codon, 8 bp of 5' untranslated region (UTR), and 239 bp of 3' UTR. The cDNA open reading frame encoded 332-amino acid with a predicted pI of 7.2 and an estimated molecular weight of 35593 Da.

Compared to the sequences in the GenBank database, Mal-cyMDH shows more than 90% identity at the amino-acid level with other plant cytosolic NAD-cyMDH, especially the dicotyledon species. Mal-cyMDH shared the highest homology (96%) with Pru-cyMDH. The similarity of Mal-cyMDH to animal and bacterial cyMDHs was also more than 50%. In addition, a highly conserved motif (IWGNH), which has been reported in all MDHs and is responsible for the catalytic activity of the dehydrogenase, and the NAD-binding motif "TGAAGQI" conserved in all cyMDHs were also present in the Mal-cyMDH amino acid sequence (Fig. 1). Hydropathy analysis revealed a strong hydrophobic domain containing about 24 amino acids downstream from the N-terminal nine amino acids (Fig. 2). This structure was also found in other cyMDHs from plants, animals and bacteria. Taken together, the conservation of these residues in our sequence strongly suggests that *Mal-cyMDH* encodes an apple cytosolic NAD-dependent MDH.

3.2 Phylogenetic tree analysis

A phylogenetic tree was constructed in order to examine the evolutionary relationships between different classes of MDHs (Fig. 3). The tree was split into two main groups. The first group included the mitochondrial (mMDH), glyoxysomal (gMDH) and part of chloroplast NAD-MDHs (cnMDHs). The second group was further divided

into two subgroups. One subgroup contained chloroplast NADP-MDHs (chMDHs), bacterial cyMDH and parts of chloroplast NAD-MDHs (cnMDHs). Another subgroup consisted of only cytosolic NAD-dependent MDHs (cyMDHs).

As to the cyMDHs from plants, mammals and bacteria, they shared an unusually high similarity of 54%–72%. The results also show that interspecies sequence similarities of the same class of MDHs exceeded intraspecies sequence similarities of the different classes of MDHs. *Arabidopsis* cyMDH shows 61% and 51% similarity with rat and bacteria cyMDH, respectively, while *Arabidopsis* cyMDH had only an 18.1% similarity with Ara-mMDH, 18.3% with Ara-gMDH and 14% with Ara-cnMDH. This indicated that MDH was a very ancestral gene which diverged to the different classes before the speciation of animals and plants (Fig. 3).

3.3 Heterologous expression of *Mal-cyMDH* in *E. coli* and enzyme activity of the fused protein

The recombinant pET30a-cyMDH was transformed into *E. coli* BL21 after confirming the correct sequence. Then it was induced by IPTG. The yields of induced expression gradually decreased during the same period along with the decline of the inducing temperature from 37°C to 16°C. While at 16°C, the yield kept elevation with prolonged inducing time (Fig. 4(a)). However, at 37°C, most of the expressed protein was in the pellet fraction, while at 16°C the majority of the expressed protein was shifted to the supernatant fraction. Furthermore, the yields of soluble protein in the supernatant were elevated by extending the inducing time (Fig. 4(b)). Finally, induction at 16°C for 24 h was selected as the best inducing conditions. The induced *E. coli* was collected and sonicated to isolate the soluble fused protein. The isolated protein was then purified by Ni-NTA His-Bind Resin of 300 mmol·L⁻¹ concentration with the highest purity (Fig. 4(c)).

The results assayed spectrophotometrically shows that the crude protein from empty pET30a or its induced product exhibited the very weak MDH activity (0.105 μmol·L⁻¹·min⁻¹·mg⁻¹Pr), while the purified fused protein had the high MDH reductive activity (133.24 μmol·L⁻¹·min⁻¹·mg⁻¹Pr) and weak oxidative activity (0.679 μmol·L⁻¹·min⁻¹·mg⁻¹Pr).

3.4 Malic acid content and MDH activity in the low- and high-acid apple fruits

The difference in malic acid content was obvious between two genotypes. The change patterns of malic acid were similar at the early stages and different at the late stages in two genotypes. Both reached the peak at 30 DAB and then gradually decreased in the low-acid genotype, while a slightly increase was noted in the high-acid at late stages which led to the markedly different levels of malic acid (Fig. 5).

Mal-cyMDH	.MAK EP VRVLVTGAAGQIGYALVPMIARG IM LGADQPVI LH LDIP PA A EA ALNGVKMELV	59
Pru-cyMDH	.MAK EP VRVLVTGAAGQIGYALVPMIARG VM LGADQPVI LH LDIP PA A EA ALNGVKMELV	59
Nic-cyMDH	.MAK EP VRVLVTGAAGQIGYALVPMIARG VM LGADQPVI LH LDIP PA A EA ALNGVKMELV	59
Zea-cyMDH	.MAK EP VRVLVTGAAGQIGYALVPMIARG VM LGADQPVI LH LDIP PA A EA ALNGVKMELV	59
Ara-cyMDH	.MAK EP VRVLVTGAAGQIGYALVPMIARG IM LGADQPVI LH LDIP PA A EA ALNGVKMELV	59
consensus	mak p rvlvtgaagqigyalvpmiarg mlgadqpvilh ldip aaealngvkmelv	
Mal-cyMDH	DAAF PL LKG VV ATTDVVEACTGVN IA VMVGGF PR KEG ME RKD VM T KN VS I YKSQ AS A LE K	119
Pru-cyMDH	DAAF PL LKG VV ATTDVVEACTGVN IA VMVGGF PR KEG ME RKD VM S KN VS I YKSQ AS A LE K	119
Nic-cyMDH	DAAF PL LKG VV ATTD AVE ACTGVN IA VMVGGF PR KEG ME RKD VM S KN VS I YKSQ AS A LE K	119
Zea-cyMDH	DAAF PL LKG VV ATTDVVEACTGVN IA VMVGGF PR KEG ME RKD VM S KN VS I YKSQ AS A LE A	119
Ara-cyMDH	DAAF PL LKG VV ATTD AVE ACTGVN IA VMVGGF PR KEG ME RKD VM S KN VS I YKSQ AS A LE K	119
consensus	daafpllkgvvattd veactgvn avmvggfprkegmerkdvm knvsiyksqasale	
Mal-cyMDH	HAA PN CKVL VV AN PAN TNALILKE FAPS I PE KN IT CL TR LD HN RAL GQ V SER L IN V Q VS DV	179
Pru-cyMDH	HAA PN CKVL VV AN PAN TNALILKE FAPS I PE KN IT CL TR LD HN RAL GQ V SER L IN V Q VS DV	179
Nic-cyMDH	HAA PN CKVL VV AN PAN TNALILKE YAPS I PE KN IS CL TR LD HN RAL GQ V SER L IN V Q VS DV	179
Zea-cyMDH	HAA PN CKVL VV AN PAN TNALILKE FAPS I PE KN IT CL TR LD HN RAL GQ V SER L IN V Q VS DV	179
Ara-cyMDH	HAA PN CKVL VV AN PAN TNALILKE FAPS I PE KN IT CL TR LD HN RAL GQ V SER L IN V Q VS DV	179
Consensus	haa nckvlvvanpantnalilke apsipekn cltrldhnralsgq serl v vsdv	
Mal-cyMDH	KN VI I W GNH SS S Q Y PD VN HAT V K T PS GE KV REL VAD DA WL NG EF IS TV Q Q R GA AI KAR	239
Pru-cyMDH	KN VI I W GNH SS S Q Y PD VN HAT V K T PS GE KAV REL VAD DA WL NG EF IS TV Q Q R GA AI KAR	239
Nic-cyMDH	KN VI I W GNH SS S Q Y PD VN HAT V AT PAGE KF REL VAD DA WL NG EF IS TV Q Q R GA AI KAR	239
Zea-cyMDH	KN VI I W GNH SS S Q Y PD VN HAT V K T ST GE KF REL VSD DE WL NG EF IS TV Q Q R GA AI KAR	239
Ara-cyMDH	KN VI I W GNH SS S Q Y PD VN HAT V K T SS GE KF REL VKN DE WL NG EF IS TV Q Q R GA AI KAR	239
Consensus	knviiwgnhss qypdvnhatv t gek vrelv d wl gefi tvqrgaaiikar	
	▲▲▲▲	
Mal-cyMDH	KL SS AL SA ASSAC DH IRD VV LT PE GT V SM GV SD GS Y D V PS GL I F S FP V TC Q H GE W KI	299
Pru-cyMDH	KL SR AL SA ASSAC DH IRD VV LT PE GT V SM GV SD GS Y N V PS GL I Y S FP V TC Q NG EW K I	299
Nic-cyMDH	KL SS AL SA ASSAC DH IRD VV LT PE GT V SM GV SD GS Y N V P AG LI Y S FP V TC Q NG EW S I	299
Zea-cyMDH	K F SSAL SA ASSAC DH IRD VV LT PE GT F SM GV SD GS Y GV PS GL I Y S FP V TC S G GE W K I	299
Ara-cyMDH	KL SS AL SA ASSAC DH IRD VV LT PE GT F SM GV SD GS Y N V P AG LI Y S FP V TC R NG EW T I	299
Consensus	k s alsaaassacdhirdvw gtpegt vsmgvysdgsy vp gli sfpv c gew i	
Mal-cyMDH	V Q GL S I D E F SR KK I D A T A E L S E E K A L A Y S C L S...	332
Pru-cyMDH	V Q GL S I D E F SR KK I D A T A E L S E E K A L A Y S C L S...	332
Nic-cyMDH	V Q GL E I D E F SR KK I D A T A E L S E E K A L A Y S C L I...	332
Zea-cyMDH	V Q GL E I D E F SR KK M D A T A E L T E E K T L A Y S C L E...	332
Ara-cyMDH	V Q GL E I D A S R KK M D L T A E L K E E K D L A Y S C L S...	332
consensus	vqgl id srkk d ta el eek layscl	

Fig. 1 Alignment of the inferred amino acid sequence of Mal-cyMDH and those of several other plants
 Note: The NAD-binding regions and catalytic motif are marked by underlines and triangles, respectively.

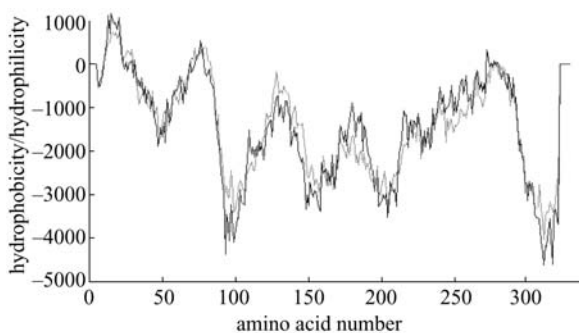


Fig. 2 Hydropathy plot analysis of the predicted polypeptide of Mal-cyMDH by TMpred program
 Note: Amino acid residues are numbered from left to right on the horizontal axes. The hydrophobic and hydrophilic positions are plotted above and below the ordinate, respectively.

cyMDH reductive activity was analyzed in low- and high-acid genotypes. Generally, cyMDH reductive activity declined and then increased gradually in 2 genotypes, except a peak at 60 DAB in the high-acid genotype. cyMDH reductive activities shows significant difference. It was much higher in the high-acid genotype than that in the low-acid one at the same stage (Fig. 6), in agreement with the difference of malic acid content between two genotypes. The much lower oxidative activities of cyMDH were detectable only at 30 and 90 DAB in the high-acid fruit and 150 DAB in the low-acid fruit (Fig. 7).

4 Discussion

In this study, *cyMDH* was isolated and characterized from apples and designated as *Mal-cyMDH*. Polygenetic analysis

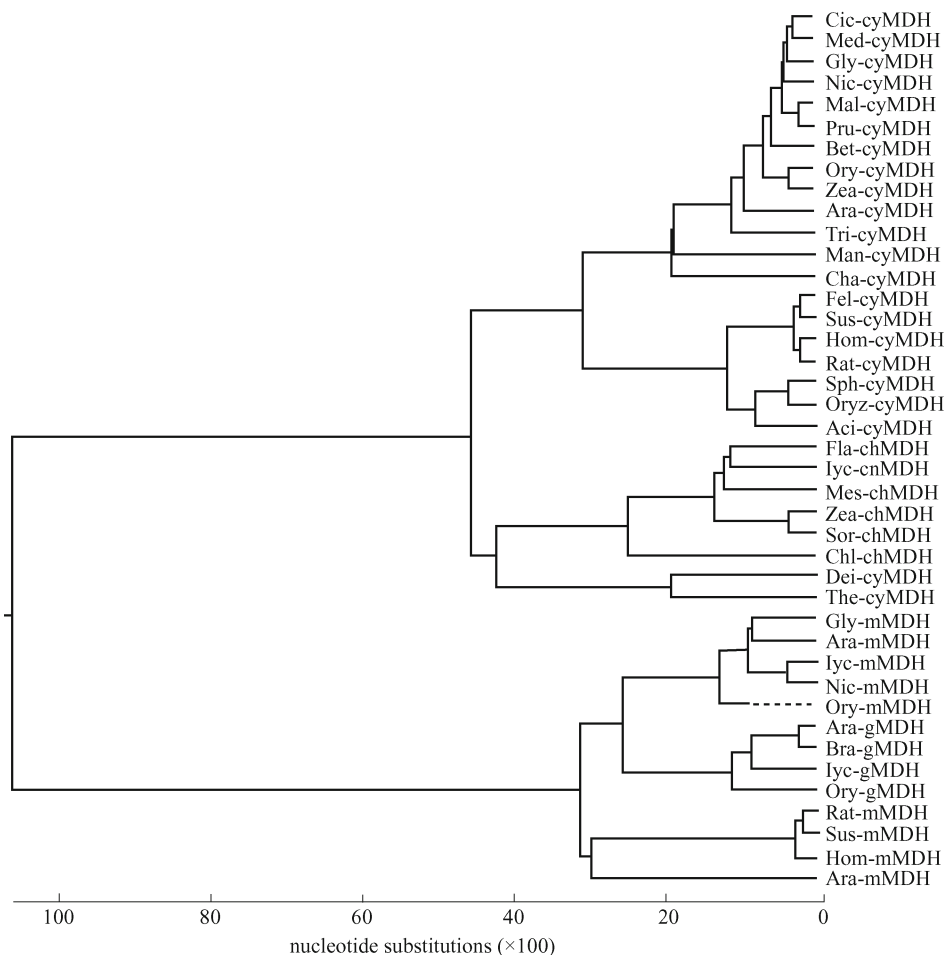


Fig. 3 Phylogenetic tree of cyMDH (Cluster W)

shows that cyMDH sequences are highly conserved in plants, animals and bacteria. Almost all *cyMDHs* could be clustered into the same subgroup. Interspecies sequence similarities of the same class of MDHs are higher than intraspecies sequence similarities of different classes of

MDHs. An explanation of the differences among MDHs from the cytosol and organelles is that a common ancestral *MDH* gene might have been duplicated before invasion to primordial eukaryotes by bacteria to produce organelles according to the probable endosymbiotic origin of these

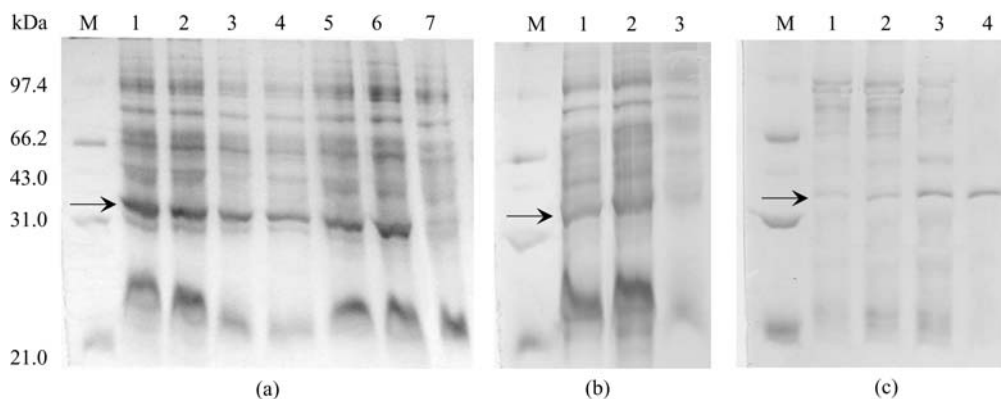


Fig. 4 SDS-PAGE of pET30a-cyMDH expression products (a), soluble protein in the supernatant (b) and recombinant proteins purified by Ni-NTA column (c)

Note: (a): 1–4 indicate the inductions at 37°C, 30°C, 22°C and 16°C for 4 h, 5–6 at 16°C for 12 h and 24 h, and 7 is for pET30a (+); (b): 1 and 2 indicate the inductions at 16°C for 12 and 24 h, and 3 at 37°C for 12 h; (c): 1–4 indicate eluted by 50, 100, 200 and 300 mmol·L⁻¹, respectively. The target fused protein was arrowed.

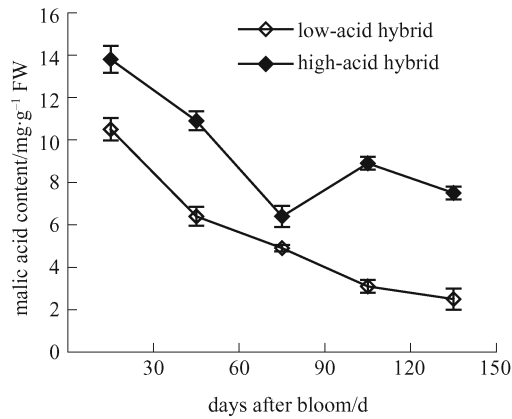


Fig. 5 Change of malic acid content during fruit development

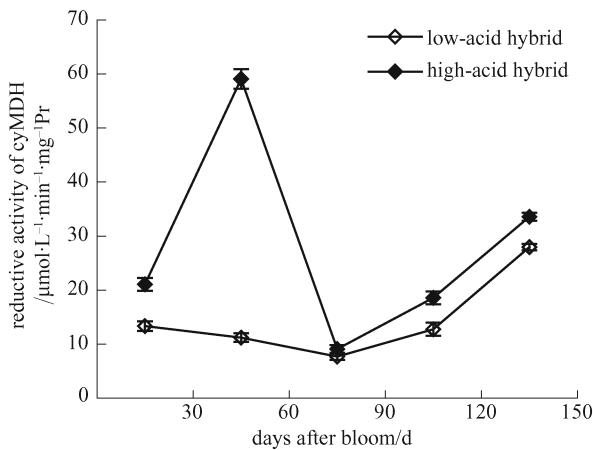


Fig. 6 Comparison of cyMDH activity between the high- and low-acid fruits

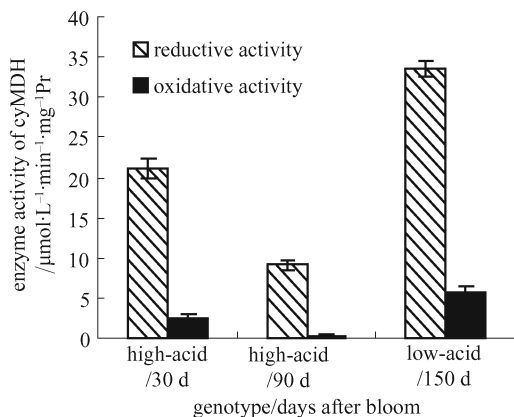


Fig. 7 Comparison of cyMDH activity between the high- and low-acid fruits

organelles (McAlister-Henn, 1998; Gray et al., 2001). Furthermore, different classes of MDH came into being before the speciation of animals and plants. Therefore, *cyMDH* is likely to represent the ancestral form of MDH,

which further evolved into other forms of MDH. However, the pattern of relatedness between MDHs is very complicated and a meaningful interpretation of the evolutionary origins of this enzyme still requires more amino acid sequence information.

Malic acid accumulation in fruits differs from other well-known fruit developmental processes, such as ripening-associated ethylene synthesis and cell wall degradation, which are associated with many highly expressed specific genes in fruit (Callahan et al., 1993). It is more complex to analyze the metabolism of malic acid as it is controlled by synthesis, degradation and transportation. The low-acid character of fruit was controlled by a major gene from the researches on apples (Visser and Verhaegh, 1978; Maliepaard et al., 1998; Yao et al., 2006), peaches (Yoshida, 1970), grapes (Boubals et al., 1971), pomelos (Cameron and Soost, 1977) and tomatoes (Stevens, 1972). The key enzymes involved in malic acid metabolism should be the most downstream factors regulated by the major gene. Here, *cyMDH* was isolated and the fused protein from prokaryotic expression confirmed that it catalyzed a reversible reaction dominated by directing malic acid synthesis. The severely weak activity of MDH in the crude protein from the empty carrier or its induced product shows that there were iso-enzymes of MDH in *E. coli*. However, the purified fused protein by His tag could eliminate its isoenzymes and assured the veracity. In addition, the clear difference of *cyMDH* activities in two genotypes implicated that *cyMDH* transcripts were likely to be different. Especially for *cyMDH*, activities in both genotypes kept increasing since 90 DAB, whereas malic acid content went on decreasing in the low-acid fruit areas, which suggested malic acid accumulation was also affected by other key enzymes apart from *cyMDH*. It is noteworthy that MDH from other organelles could not be eliminated. However, it would have some effects on only the absolute values of enzyme activity rather than no effects on the comparison between two genotypes.

The clear relationship between *cyMDH* expression and malic acid accumulation awaits further investigation. It is our next target to acquire the high-acid processing apple by gene transformation.

References

Basil H, Edgar L P, Teixeira A, Christian R, Shabanowitz J, Hunt D, Klotman P (2002). Cytosolic malate dehydrogenase confers selectivity of the nucleic acid-conducting channel. *PNAS*, 99: 1707–1712

Boubals D, Bourzeix M, Guitraud J (1971). Gora Chirine, an Iranian cv. with a low berry acid levels. *Ann Amelior Plantes*, 21: 281–285

Bradford M (1976). A rapid and sensitive method for the quantitation of microgram quantities of protein utilizing the principle of protein-dye binding. *Anal Biochem*, 72: 248–254

- Callahan A M, Morgens P H, Cohen R A (1993). Isolation and initial characterization of cDNAs for messenger RNAs regulated during peach fruit development. *J Am Soc Hortic Sci*, 118: 531–537
- Cameron J W, Soost R K (1977). Acidity and total soluble solids in *Citrus* hybrids and advanced crosses involving acidless orange and acidless pummelo. *J Am Soc Hortic Sci*, 102: 198–201
- Chollet R, Vidal J, O'Leary M H (1996). Phosphoenolpyruvate carboxylase: a ubiquitous, highly regulated enzyme in plants. *Annu Rev Plant Physiol Plant Mol Biol*, 47: 273–298
- Christelle E, Moinga A, Dirlwangera E, Raymond P, Monet R, Rothan C (2002). Isolation and characterization of six peach cDNAs encoding key proteins in organic acid metabolism and solute accumulation: involvement in regulating peach fruit acidity. *Physiol Plant*, 114: 259–270
- Gibson N, McAlister-Henn L (2003). Physical and genetic interactions of cytosolic malate dehydrogenase with other gluconeogenic enzymes. *The Journal of Biological Chemistry*, 278: 25628–25636
- Gray M W, Burger G, Lang B F (2001). The origin and early evolution of mitochondria. *Genome Biol*, 2: 10181–10185
- Hanning I, Heldt H W (1993). On the function of mitochondrial metabolism during photosynthesis in spinach (*Spinacia oleracea* L.) leaves. *Plant Physiol*, 103: 1147–1154
- Kromer S, Heldt H W (1991). Respiration of pea leaf mitochondria and redox transfer between the mitochondrial and extramitochondrial compartment. *Biochim Biophys Acta*, 1057: 42–50
- Maliepaard C, Alston F H, Arkel G V, Brown L M, Chevreau E, Dunemann F, Evans K M, Gardiner S, Guilford P, Heusden A W, Janse J, Laurens F, Lynn J R, Manganaris A G, Periam N, Rikkerink E, Roche P, Ryder C, Sansavini S, Schmidt H, Tartarini S, King G J (1998). Aligning male and female linkage maps of apple (*Malus pumila* Mill.) using multi-allelic markers. *Theor Appl Genet*, 97: 60–73
- McAlister-Henn L (1988). Evolutionary relationships among the malate dehydrogenases. *Trends Biochem Sci*, 13: 178–181
- Stevens M A (1972). Citrate and malate concentration in tomato fruits: Genetic control and maturational effects. *J Am Soc Hortic Sci*, 97: 655–658
- Visser T, Verhaegh J J (1978). Inheritance and selection of some fruit characters of apple. 1. Inheritance of low and high acidity. *Euphytica*, 27: 753–760
- Yao Y X, Zhai H, Zhao L L, Yi K, Liu Z, Song Y (2006). Analysis of apple fruit acid/low-acid trait by SSR marker. *Acta Horticulturae Sinica*, 33(2): 244–248 (in Chinese)
- Yao Y X, Zhao L L, Hao Y J, Zhai H (2005). Effective extraction of total RNA in apple flesh with improved hot borate method. *Journal of Fruit Science*, 22(6): 737–740 (in Chinese)
- Yoshida M (1970). Genetical studies on the fruit quality of peach varieties. I Acidity. *Bull Hortic Res Stn Jpn, Series A*, 9: 1–15
- Yu D, Ma Q H (2004). Characterization of a cytosolic malate dehydrogenase cDNA which encodes an isozyme toward oxaloacetate reduction in wheat. *Biochimie*, 86: 509–518